Peremennye Zvezdy (*Variable Stars*) **44**, No. 11, 2024

Received 25 November; accepted 2 December.

DOI: 10.24412/2221-0474-2024-44-131-138

The Apsidal Motion in the Eclipsing Binary V1437 Cas

V. S. Kozyreva[1], A. I. Bogomazov[1], F. B. Khamrakulov[2,3]

[1] Lomonosov Moscow State University, Sternberg Astronomical Institute, 119234, Universitetskij prospect, 13, Moscow, Russia

[2] Ulugh Beg Astronomical Institute of the Academy of Sciences of the Republic of Uzbekistan, 100052, Astronomicheskaya str., 33, Tashkent, Uzbekistan

[3] Samarkand State University, 140104, University blv., 15, Samarkand, Uzbekistan

We estimated the apsidal motion rate in the eclipsing binary system V1437 Cas using TESS light curves as $\mathrm{d}\omega/\mathrm{d}t = 0\overset{\circ}{.}252 \pm 0\overset{\circ}{.}025$ yr^{-1}. Existing TESS light curves of the system contain 4 extremely deep minima of unknown nature.

1 Introduction

The eclipsing binary V1437 Cas (TIC 314039042, NSV 14400) was found by Nielsen (1936) on photographic plates. Its characteristics were not specified. Later observations made it possible to determine the variability type for this system and to derive its orbital period $P_{\mathrm{orb}} = 3\overset{\mathrm{d}}{.}34363$ (Kazarovets 2021). After that, the star was included into the General Catalogue of Variable Stars as V1437 Cas (Kazarovets et al. 2023).

In 2015–2018, the ZTF project (Bellm et al. 2019) obtained observations[1] of V1437 Cas. These ZTF data are not well suited to find times of minima from individual light curves, all of them being in the form of separated pieces of light curves with gaps of ≈ 1 day. The photometric uncertainty is about $0\overset{\mathrm{m}}{.}03$; such data cannot be used to determine the change of the position of the secondary minimum, with respect to the primary minimum, with time.

The data obtained by the TESS satellite[2] are suitable in order to derive the apsidal motion rate of the object under our study. The satellite observed it[3] in 2019, 2020, 2022 and 2024, the precision of different sets of observations differs significantly. The average error in 2019 and 2020 was 0.0044 mag, in 2022 it was 0.009 mag, in 2024 it was 0.012 mag.

The star is a semi-detached binary with a flat plateau between minima. This can be seen in Fig. 1 that shows a TESS light curve of the system in 2019, minima I and II. Along the horizontal axis, we plot phases calculated using Eq. 1; the phase of the secondary minimum (Min II) with respect to the phase of primary minimum (Min I) is

[1] Data can be downloaded from https://irsa.ipac.caltech.edu/cgi-bin/Gator/nph-scan?mission=irsa&submit=Select&pro-jshort=ZTF

[2] Data can be downloaded from https://mast.stsci.edu/portal/Mashup/Clients/Mast/Portal.html

[3] Files from MAST archive:
hlsp_qlp_tess_ffi_s0017-0000000314039042_tess_v01_llc.fits,
hlsp_qlp_tess_ffi_s0024-0000000314039042_tess_v01_llc.fits,
hlsp_qlp_tess_ffi_s0057-0000000314039042_tess_v01_llc.fits,
hlsp_qlp_tess_ffi_s0077-0000000314039042_tess_v01_llc.fits

0.6504. Along the vertical axis, we show the brightness of the star normalized to that outside minima.

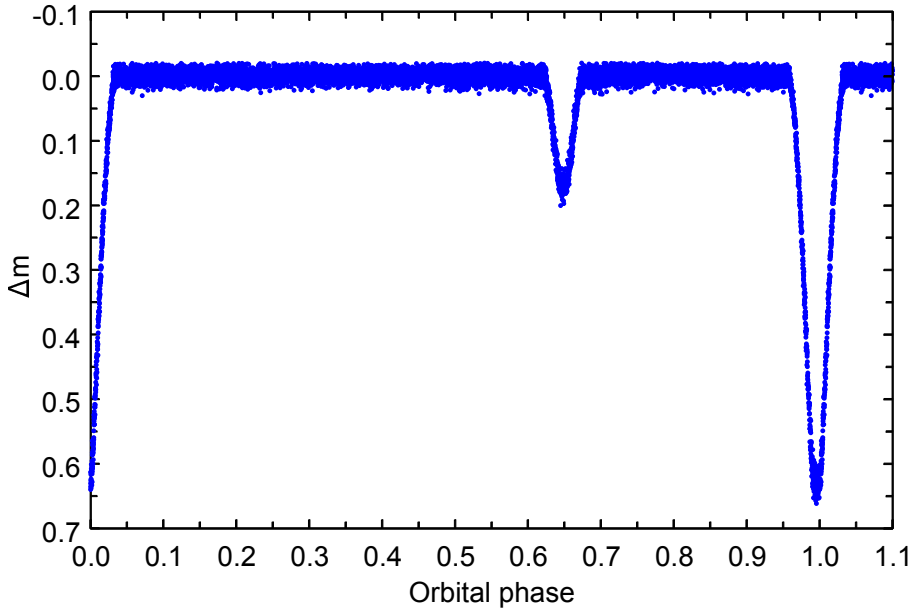

Figure 1.
A sample TESS light curve of V1437 Cas in 2019.

To find parameters of the system, we used a program based on the model of spherical stars with a linear limb darkening (Khaliullina & Khaliullin 1984). The program calculates radii of stars, their luminosities (including a third light), eccentricity, periastron longitude and inclination of the orbit. As a parameter, the program also is able to compute the time of primary minimum and coefficients of limb darkening (Kozyreva & Zakharov 2006). A free search of limb darkening coefficients was used to calculate the coefficient for the primary star for observations in 2019 and 2020. Observations in 2022 and 2024 have, respectively, twice and three times larger uncertainties, therefore we did not calculate the coefficient in the 2022 and 2024 solutions but used a fixed value.

The secondary minimum is too small, therefore the precision of observations was not sufficient to reliably find the limb darkening coefficient of the secondary star. We used a theoretical value of limb darkening coefficient for the secondary star (van Hamme 1993) according to the assumed temperature of the star and to the spectral band of TESS observations. To find the temperature of the secondary star, we used the dependence between the temperature and surface brightness of the star.

The catalogue by Pickles (1998) contains the following parameters for the object under study: the spectral type is A5V and the effective temperature is $T_{\rm eff} = 8492$ K. Later catalogues, such as the TESS input catalogue (Stassun et al. 2019), ATLAS-REFCAT2 (Tonry et al. 2018) and Gaia DR2 (Bai et al. 2019), give different values of $T_{\rm eff}$ for the primary component of V1437 Cas: respectively, $T_{\rm eff} = 8220$ K, $T_{\rm eff} = 7330$ K, $T_{\rm eff} = 8115$ K.

The value of the limb darkening coefficient in our solution (primary star, Table 1) is close to the theoretical one (van Hamme 1993) for a star with $T_{\rm eff} = 8500$ K and with the star's temperature in the catalogue by Pickles (1998). If this temperature is assumed to be the temperature of the primary star, then the temperature of the secondary star can be found using the Stephan–Boltzmann law and the ratio of surface brightnesses of the

Table 1: Parameters of stars and orbital elements calculated using TESS light curves in 2019, 2020, 2022 and 2024.

Parameter	"2019"	"2020"	"2022"	"2024"
r_1	0.1251±0.0025	0.1247±0.0025	0.1226±0.0025	0.1231±0.0030
r_2	0.0855±0.0030	0.0858±0.003	0.0849±0.004	0.0868±0.0040
i, °	88.4±0.4	88.5±0.3	88.8±0.3	89.6±0.3
e	0.2932±0.0015	0.2943±0.0015	0.2970±0.0040	0.2898±0.0040
ω, °	323.65±0.04	323.47±0.04	323.33±0.03	326.10±0.03
L_1	0.857±0.005	0.855±0.005	0.857±0.007	0.835±0.007
L_2	0.139±0.005	0.144±0.005	0.143±0.007	0.143±0.007
L_3	0.004±0.003	0.001±0.002	0.000±0.020	0.02±0.010
u_1	0.36±0.02	0.38±0.02	0.37 (fixed)	0.37 (fixed)
u_2	0.47 (fixed)	0.47(fixed)	0.47(fixed)	0.47(fixed)
J_1/J_2	2.88±0.02	2.84±0.02	2.87±0.02	2.90±0.02
σ	0.005	0.005	0.011	0.014

Table 2: The periastron longitude for TESS light curves in 2019, 2020, 2022, 2024 and for the ZTF light curve calculated with fixed parameters of the "2019" light curve (Table 1).

Parameter	"2019"	"2020"	"2022"	"2024"	ZTF
ω, °	323.65±0.04	323.81±0.04	324.56±0.07	324.83±0.04	323.15±0.10
E_0	JD 2458776.01	2458970.66	2459867.60	2460404.71	2457816.02

two stars (Table 1):

$$\frac{J_1}{J_2} = \frac{L_1}{L_2}\frac{r_2^2}{r_1^2}, \tag{1}$$

where J_1 and J_2 are the surface brightnesses of the primary and secondary stars, L_1 and L_2 are their luminosities, r_1 and r_2 are their radii.

The temperature of the secondary from Eq. 1 is 5880 K. The theoretical limb darkening coefficient for such a temperature is 0.47 (van Hamme 1993); in our solution, we use this value for the secondary star. Table 1 shows solutions for system's elements that have been found in a free search for all parameters except limb darkening coefficients. These solutions correspond to light curves obtained in 2019, 2020, 2022, and 2024. The parameters are very similar in all these solutions. In Table 1, i is the inclination of the orbit; e is the eccentricity of the orbit; ω is the ascending node longitude; $u_{1,2}$ are the limb darkening coefficients, respectively for the primary and the secondary; σ is the standard deviation; $L_{1,2,3}$ are the luminosities, respectively of the primary, secondary, and third light in units of the total luminosity of the system; $r_{1,2}$ are the radii of the primary and secondary in units of the semi-major axis of the system.

For subsequent calculations, we assumed that radii and luminosities of the stars and the orbital inclination had not changed during TESS observations. This supposition made it possible to find the periastron longitude for different epochs and to determine the apsidal motion rate from these calculations. Table 2 shows the periastron longitude computed with all other parameters fixed (using the solution for the 2019 light curve, Table 1). In Table 2, E_0 is the average epoch of the values of ω in corresponding sets of observations.

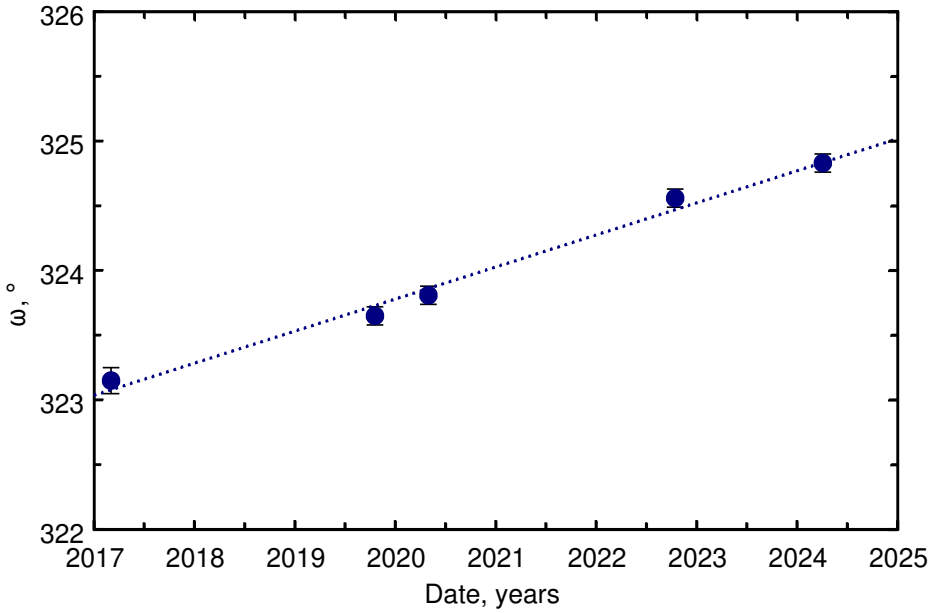

Figure 2.
The periastron longitude versus time. The first (2017) data point corresponds to results derived from ZTF light curves, the other data points are results derived from TESS light curves. See Table 2.

Figure 2 shows the dependence of the periastron longitude on time for solutions that correspond to TESS light curves in 2019, 2020, 2022, 2024 (Table 2) and to the ZTF observations. The linear dependence can be seen, the least square method gives the solution with 10% uncertainty:

$$\frac{\mathrm{d}\omega}{\mathrm{d}t} = 0.252^\circ \pm 0.025^\circ\,\mathrm{yr}^{-1}, \tag{2}$$

$$U_{\mathrm{aps}} = (1430 \pm 140)\,\mathrm{yr}, \tag{3}$$

where $\mathrm{d}\omega/\mathrm{d}t$ is the apsidal motion rate, U_{aps} is the period of the apsidal motion.

Times of minima derived from TESS observations are collected in Table 3. The time of the primary minimum is one of the parameters that can be found in free search in a light curve solution along with other parameters. The time of the secondary minimum is obtained in the mode of search for only this parameter with the remaining parameters fixed at the values derived for the free search option. The differences between observed (O) and calculated (C) times for primary (I, $(\mathrm{O–C})_1$) and secondary (II, $(\mathrm{O\text{-}C})_2$) minima (Table 3) were calculated using the ephemerides:

$$\mathrm{C}_1 = \mathrm{HJD}\,2458406.8817 + (3\overset{\mathrm{d}}{.}3437039 \pm 0\overset{\mathrm{d}}{.}0000002) \times E_1, \tag{4}$$

$$\mathrm{C}_2 = \mathrm{HJD}\,2458409.0577 + (3\overset{\mathrm{d}}{.}3437039 \pm 0\overset{\mathrm{d}}{.}0000002) \times E_2. \tag{5}$$

The displacement of (O–C) deviations of the primary and secondary minima with respect to each other (Fig. 3) usually can be explained with apsidal motion. Due to this motion, periods of primary and secondary minima are different. A short time interval of observations in comparison with the period of apsidal motion and a lucky orientation of the periastron with respect to the observer make it possible to describe (O–C) with a linear formula. New ephemerides calculated using the least square method are as follows:

Table 3: Times of primary and secondary minima of V1437 Cas derived from TESS light curves obtained in 2019, 2020, 2022 and 2024.

Min I BJD	$(O–C)_1$ days	$(O–C)_2$ days	Min II BJD	$(O–C)_1$ days	$(O–C)_2$ days
2458768.0013	–0.0007	0.0001	2458770.1787	0.0008	0.0001
2458771.3446	–0.0011	–0.0003	2458773.5213	–0.0002	–0.0010
2458774.6886	–0.0008	0.0000	2458780.2101	0.0012	0.0004
2458778.0313	–0.0017	–0.0009	2458783.5526	–0.0017	–0.0009
2458781.3761	–0.0006	0.0002	2458786.8972	0.0009	0.0001
2458784.7195	–0.0009	-0.0001	2458960.7704	0.0015	0.0003
2458788.0636	–0.0005	0.0003	2458964.1141	0.0015	0.0003
2458958.5920	–0.0010	0.0002	2458967.4577	0.0014	0.0002
2458961.9357	–0.0010	0.0002	2458970.8020	0.0020	0.0008
2458965.2793	–0.0011	0.0001	2458974.1450	0.0013	0.0001
2458971.9666	–0.0012	0.0000	2458977.4889	0.0014	0.0002
2458975.3103	–0.0012	0.0000	2458980.8319	0.0007	–0.0005
2458978.6542	–0.0010	0.0002	2459853.5410	0.0033	0.0002
2458981.9973	–0.0016	-0.0004	2459856.8840	0.0026	–0.0005
2459854.7025	–0.0030	0.0001	2459860.2288	0.0037	0.0006
2459858.0460	–0.0032	-0.0001	2459866.9155	0.0030	–0.0001
2459861.3891	–0.0038	-0.0007	2459870.2591	0.0029	–0.0002
2459868.0775	–0.0028	0.0004	2459873.6034	0.0035	0.0004
2459871.4208	–0.0032	0.0000	2459876.9462	0.0026	–0.0005
2459878.1082	–0.0032	-0.0001	2459880.2902	0.0029	–0.0002
2459881.4520	–0.0032	0.0000	2460398.5656	0.00432	0.00012
2460396.3815	–0.0039	0.0004	2460401.9103	0.00528	0.00108
2460399.7255	–0.0036	0.0007	2460405.2525	0.00383	–0.00038
2460403.0691	–0.0037	0.0006	2460418.6288	0.00528	0.00104
2460406.4131	–0.0034	0.0009	2460421.9726	0.00538	0.00113
2460419.7878	–0.0035	0.0008			
2460423.1318	–0.0032	0.0011			

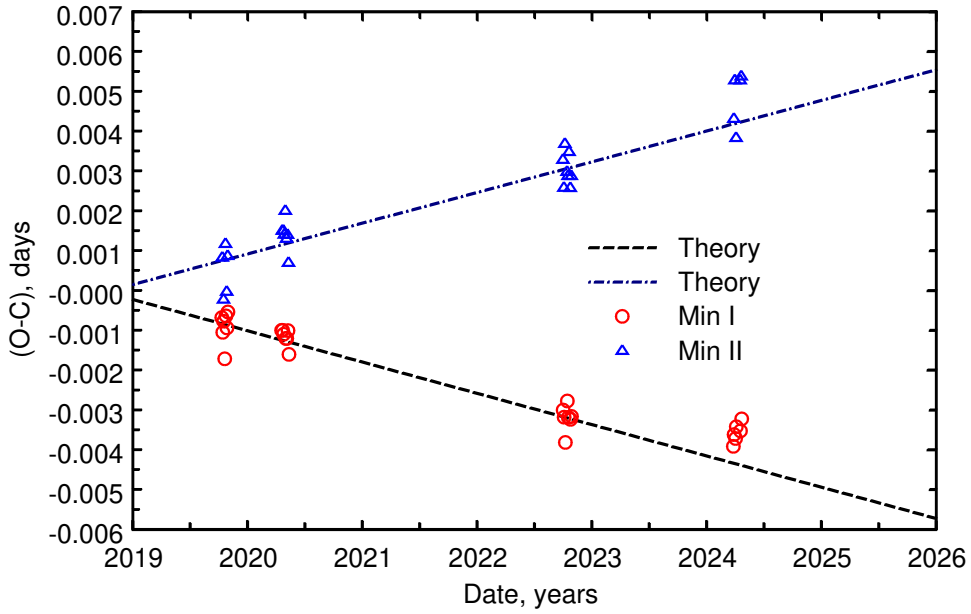

Figure 3.
(O–C) values for V1437 Cas calculated using ephemerides (4) and (5).

$$\mathrm{C}_1 = \mathrm{HJD}\,(2458406.8822 \pm 0.0002) + (3\overset{\mathrm{d}}{.}3436969 \pm 0\overset{\mathrm{d}}{.}0000003) \times E_1, \tag{6}$$

$$\mathrm{C}_2 = \mathrm{HJD}\,(2458409.0577 \pm 0.0003) + (3\overset{\mathrm{d}}{.}3437119 \pm 0\overset{\mathrm{d}}{.}0000003) \times E_2. \tag{7}$$

The difference between the periods for secondary and primary minima is $P_2 - P_1 = 1.74 \pm 0.17$ s. The equation by Rudkjøbing (1959) relates the difference between periods of primary and secondary mimina to the apsidal motion rate:

$$\frac{dP}{P} = 2P(1-e^2)^{\frac{3}{2}} e \sin\omega \frac{d\omega}{dt} \frac{1}{\pi(1-e^2\sin^2\omega)}. \tag{8}$$

For the difference between periods for primary and secondary minima 1.74 ± 0.17 s, the corresponding apsidal motion rate is:

$$\frac{d\omega}{dt} = 0.286^\circ \pm 0.03^\circ\,\mathrm{yr}^{-1}.$$

This rate is in a satisfactory agreement with that calculated above (Eq. 2).

To compare theoretical and observational values of the apsidal motion rate, it is necessary to know parameters of the stars. The most important parameters are masses and temperatures of the components. If the temperature of the primary is assumed to be 8500 K, then (taking into account the ratio of surface brightnesses of the stars), the temperature of the secondary, according to the Stephan–Boltzmann law, should be 5880 K (see above). Masses of main sequence stars with such temperatures should be $2.50M_\odot$ and $1.07M_\odot$, respectively (see Fig. 9 in Eker et al. 2018). Using these input parameters, we estimated theoretical values of the stellar internal structure coefficients k_2 (Sterne, 1939) from tables by Claret & Gimenez (1989). The apsidal motion rate obtained from theory and from observations is the same inside its uncertainty interval, the values of k_2 are as follows: $k_2^1 = 0.0020$, $k_2^2 = 0.0134$. These quantities can be obtained for the effective temperature of the primary star 8500 K; for another temperature, the result can be different.

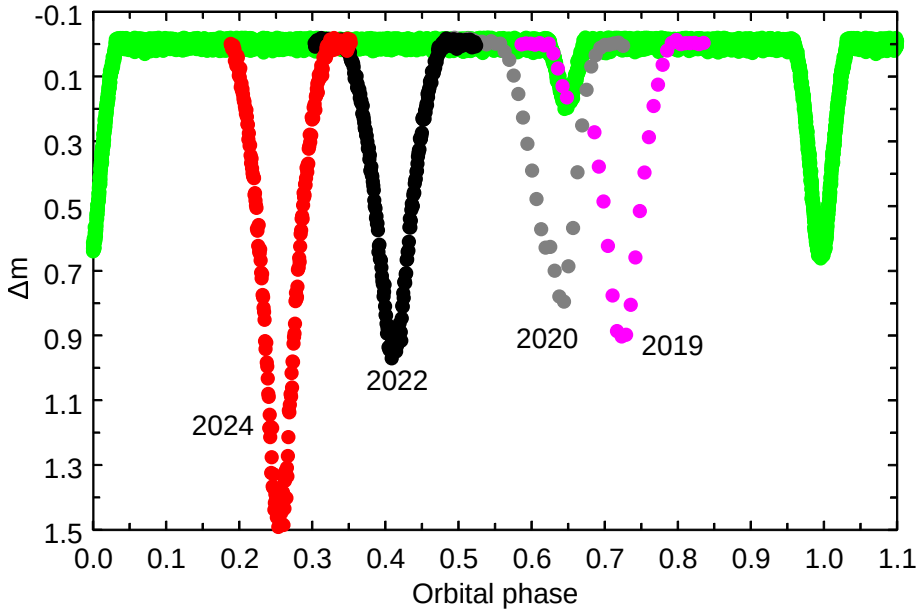

Figure 4.
Extremely deep minima of V1437 Cas.

Table 4: Extremely deep minima of V1437 Cas found in TESS observations.

Time of minimum BJD	Year	Depth mag	Duration days
2458767.081±0.015	2019	0.90±0.01	0.439±0.012
2458957.405±0.020	2020	0.80±0.01	0.451±0.015
2459856.080±0.015	2022	0.92±0.01	0.447±0.012
2460400.583±0.015	2024	1.45±0.01	0.450±0.012

The system has an interesting peculiarity in its TESS light curves. In each set of TESS observations (2019, 2020, 2022, 2024), there is one extremely deep minimum at different phases. Such extreme minima are deeper than the primary minimum by more than $0\overset{m}{.}25$, and their widths are also larger by a factor of ≈ 1.5 (see Table 4 and Fig, 4). The orbital phases of the binary are plotted along the abscissa of Fig. 4. The shape of extremely deep minima in 2019, 2022, and 2024 is almost symmetric. The shape of minimum in 2020 is non-symmetric, its position in the light curve coincides with the secondary minimum of the system. Times of minima in 2019, 2022, and 2024 supposedly have a period $27\overset{d}{.}255 \pm 0\overset{d}{.}001$. With this period, the deep minimum of 2020 should happen 8 hours later than it was observed. Probably, both stars can be eclipsed by a dark body (e.g., a comet, a disk around a planet/brown dwarf). Alternatively, these minima can arise from TESS hardware noise. At least, earlier we did not see anything similar in other light curves of other eclipsing binary stars (including TESS light curves, e.g., the light curves of FL Lyr, Kozyreva et al. 2023).

Acknowledgments

This research has made use of the SIMBAD database (operated at CDS, Strasbourg, France) and of NASA's Astrophysics Data System. Some of the data presented in this

paper were obtained from the Mikulski Archive for Space Telescopes (MAST).

References:

Bai, Y., Liu, J., Bai, Z. et al. 2019, *Astron. J.*, **158**, No. 2, id. 93
Bellm, E. C., Kulkarni, S. R., Graham, M. J., et al. 2019, *Publ. Astron. Soc. Pacific*, **131**, 018002
Claret, A. & Gimenez, A., 1989, *Astron. & Astrophys., Suppl. Ser.*, **81**, No. 1, 37
Eker, Z., Bakiş, V., Bilir, S., et al. 2018, *Monthly Notices Roy. Astron. Soc.*, **479**, 5491
Kazarovets, E. V., 2021, *Perem. Zvezdy Prilozh. / Var. Stars Suppl.*, **21**, No. 2
Kazarovets, E. V., Samus, N. N., Durlevich, O. V., et al. 2023, *Perem. Zvezdy / Var. Stars*, **43**, No. 9, 101
Khaliullina, A. I. & Khaliullin, K. F. 1984, *Soviet Astron.*, **28**, No. 2, 228
Kozyreva, V. S., Bogomazov, A. I., Demkov, B. P. et al. 2023, *Astron. Rep.*, **67**, No. 5, 483
Kozyreva, V. S. & Zakharov, A. I. 2006, *Astron. Lett.*, **32**, No. 5, 313
Nielsen, A. V. 1936, *Astron. Nachr.*, **261**, 7
Pickles, A. J. 1998, *Publ. Astron. Soc. Pacific*, **110**, 863
Rudkjøbing, M. 1959, *Ann. d'Astrophys.*, **22**, No. 2, 111
Stassun, K. G., Oelkers, R. J., Paegert, M., et al. 2019, *Astron. J.*, **158**, No. 4, id. 138
Sterne, T. E. 1939, *Monthly Notices Roy. Astron. Soc.*, **99**, 662
Tonry, J. L., Denneau, L., Flewelling, H., et al. 2018, *Astrophys. J.*, **867**, No. 2, id. 105
van Hamme, W. 1993, *Astron. J.*, **106**, No. 5, 2096